Title
Alisol B 23-acetate attenuates CKD progression by regulating the renin–angiotensin system and gut–kidney axis

Authors
Chen, Hua
Wang, Min-Chang
Chen, Yuan-Yuan
et al.

Publication Date
2020

DOI
10.1177/2040622320920025

Peer reviewed

Ther Adv Chronic Dis
2020, Vol. 11: 1–21
DOI: 10.1177/2040622320920025

Alisol B 23-acetate attenuates CKD progression by regulating the renin–angiotensin system and gut–kidney axis

Hua Chen*, Min-Chang Wang*, Yuan-Yuan Chen, Lin Chen, Yan-Ni Wang, Nosratola D. Vaziri, Hua Miao and Ying-Yong Zhao

Abstract

Background: Increasing evidence suggests a link between the gut microbiome and various diseases including hypertension and chronic kidney disease (CKD). However, studies examining the efficacy of controlling blood pressure and inhibiting the renin–angiotensin system (RAS) in preventing CKD progression are limited.

Methods: In the present study, we used 5/6 nephrectomised (NX) and unilateral ureteral obstructed (UUO) rat models and cultured renal tubular epithelial cells and fibroblasts to test whether alisol B 23-acetate (ABA) can attenuate renal fibrogenesis by regulating blood pressure and inhibiting RAS.

Results: ABA treatment re-established dysbiosis of the gut microbiome, lowered blood pressure, reduced serum creatinine and proteinuria, suppressed expression of RAS constituents and inhibited the epithelial-to-mesenchymal transition in NX rats. Similarly, ABA treatment inhibited expression of collagen I, fibronectin, vimentin, α-smooth muscle actin and fibroblast-specific protein 1 at both mRNA and protein levels in UUO rats. ABA was also effective in suppressing activation of the transforming growth factor-β (TGF-β)/Smad3 and preserving Smad7 expression in both NX and UUO rats. *In vitro* experiments demonstrated that ABA treatment inhibited the Wnt/β-catenin and mitochondrial-associated caspase pathways.

Conclusion: These data suggest that ABA attenuated renal fibrosis through a mechanism associated with re-establishing dysbiosis of the gut microbiome and regulating blood pressure, and Smad7-mediated inhibition of Smad3 phosphorylation. Thus, we demonstrate ABA as a promising candidate for treatment of CKD by improving the gut microbiome and regulating blood pressure.

Keywords: alisol B 23-acetate, chronic kidney disease, gut microbiome, hypertension, renal fibrosis, renin–angiotensin system

Received: 9 November 2019; revised manuscript accepted: 18 March 2020.

Correspondence to:
Ying-Yong Zhao
Faculty of Life Science & Medicine, Northwest University, No. 229 Taibai North Road, Xi'an, Shaanxi 710069, China
zyy@nwu.edu.cn; zhaoyybr@163.com

Hua Chen
Yuan-Yuan Chen
Lin Chen
Yan-Ni Wang
Hua Miao
Faculty of Life Science & Medicine, Northwest University, Xi'an, Shaanxi, China

Min-Chang Wang
Instrumental Analysis Center, Xi'an Modern Chemistry Institute, Xi'an, Shaanxi, China

Nosratola D. Vaziri
Division of Nephrology and Hypertension, School of Medicine, University of California Irvine, CA, USA

*Hua Chen and Min-Chang Wang are joint first authors.

Introduction

Chronic kidney disease (CKD) is a worldwide public health problem that leads to increased risk of cardiovascular disease (CVD), end-stage renal disease (ESRD) and death. Hypertension is a risk factor for CVD and ESRD, and lowering blood pressure reduces the risk of CVD and all-cause mortality.[1] In the past two decades, angiotensin-converting-enzyme inhibitors (ACEI) and angiotensin receptor blockers (ARB) have been recommended as first-line therapy for hypertension in CKD patients.[2] Experimental and clinical studies have shown that inhibition of the renin–angiotensin system (RAS) by ACEI or

ARB in CKD patients can reduce blood pressure and proteinuria, and impede the progression of CKD to ESRD.[3] However, these agents have limited efficacy for the following reasons: (1) administration of ACEI and ARB triggers compensatory upregulation of renin, which subsequently binds to pro-renin/renin receptors and initiates a profibrotic response through an angiotensin-independent mechanism; (2) ACEI or ARB administration results in the upregulation of angiotensin II and aldosterone; and (3) intrarenal RAS remains activated when systemic RAS is fully blocked.[4] In addition, studies have demonstrated that ACEI and ARB combination therapy is not more effective than monotherapy.[5] As such, there is an urgent need to identify new RAS-inhibiting strategies to prevent/impede the progression of CKD more effectively.

There has been a trend to develop drugs that can target multiple RAS elements capable of modulating the signaling pathways that are dysregulated in patients with CKD and cardiovascular disorders. RAS activation triggers upregulation of some important fibrogenic cytokines, including transforming growth factor-β (TGF-β). TGF-β1 can activate renal interstitial fibroblasts and the renal epithelial-to-mesenchymal transition (EMT), two cellular events that are critical for the development of tubulointerstitial fibrosis (TIF).[6] The fibrogenic effects of TGF-β occur through its interaction with TGF-β receptors and subsequent activation of Smad3. Activated Smad3, together with Smad4, is translocated to the nucleolus, where it drives expression of TGF-β1-responsive genes. RAS can also induce EMT *via* activation of TGF-β/Smad-independent pathways.[6] A recent study indicates that activation of the Wnt/β-catenin pathway increases expression of RAS components and accelerates renal fibrosis.[7]

Recently, gut microbiota have been shown to play an important role in host health status.[8] The microbiota that colonises the human body has been revisited as 'a forgotten organ', owing to its influence on human health and disease. Crosstalk between the gut microbiota and its host has drawn considerable attention due to the involvement of the gut microbiota in diverse diseases including CKD, CVD and hypertension.[9,10] Emerging evidence suggests that probiotics and prebiotics can re-establish symbiosis of gut microbiota in CKD and CVD and regulate blood pressure.[11–13] Probiotics are living organisms ingested through food or supplements that can promote the health status of the host. Prebiotics are non-digestible carbohydrates that selectively stimulate the growth and activity of beneficial gut bacteria such as Bifidobacteria in the colon.[14] Recently, we reviewed natural products as a source for antifibrosis therapy and identified many natural small molecules that protect against fibrosis.[15] Increasing evidence indicates that some natural small molecules protect against renal fibrosis.[16–18] *Alisma orientale* is a well-known natural product that exhibits diuretic and anti-TIF effects,[19–22] and has been widely used for CKD treatment. Recently, we isolated the triterpenoid compound alisol B 23-acetate (ABA) from *A. orientale* using a bioactivity-directed approach.[23] The present study was undertaken to test whether ABA can protect against TIF by regulating crosstalk between the gut microbiome and RAS in 5/6 nephrectomised (NX) and unilateral ureteral obstructed (UUO) rats. In addition, we also examine the effect of ABA on the EMT of cultured renal tubular cells.

Materials and methods

Animal models and ethics approval

This study was approved by the Committee on the Ethics of Animal Experiments of the Northwest University (No. SYXK2010-004) and all procedures were conducted in accordance with the Declaration of Helsinki. Male Sprague-Dawley rats (6–8 weeks old, 180–200 g) were purchased from the Central Animal Breeding House of Fourth Military Medical University (Xi'an, Shaanxi, China). Rats were provided with food and water *ad libitum* and housed in plastic cages (⩽5 rats per cage) in a specific-pathogen-free air-conditioned vivarium with 40–70% humidity at 22 ± 2°C and 12 h light/12 h dark cycle. They were acclimatised to their housing environment for 7 days prior to experimentation, and to the experimental room for 1 h before experiments. All studies involving animals were performed in accordance with the ARRIVE guidelines for reporting experiments involving animals. NX and UUO rats were used to evaluate the therapeutic effects of ABA. All surgeries were performed under urethane anaesthesia and efforts were made to minimise suffering.

NX rats were assigned randomly to five groups ($n=7$): sham, NX, NX+ABA (5 mg/kg), NX+ABA (10 mg/kg) and NX+ABA (20 mg/kg). After intraperitoneal injection of sodium pentobarbital anaesthetic (3%, 10 mL/kg), NX rats underwent surgical resection of 2/3 of the right kidney, followed by the removal of the left kidney 1 week later. The sham group received a laparotomy only. Treatment was carried out from the ninth to the twelfth week as indicated. The sham group was given water. Under general anaesthesia, the sham, NX and treated rats were sacrificed on the twelfth week.

UUO rats were assigned randomly to three groups ($n=7$): sham, UUO and UUO + ABA (10 mg/kg). UUO was performed using our established protocol.[24] The sham, UUO and treated rats were sacrificed on the first and second weeks. Kidney tissues were collected for Western blotting, co-immunoprecipitation (Co-IP), quantitative real-time PCR and immunofluorescence analyses. Serum and urine were collected for chemical analyses.

Renal function and blood pressure

Serum creatinine and urea, as well as urine creatinine and protein, were measured using an Olympus AU6402 automatic analyser. Creatinine clearance was calculated. Blood pressure was measured weekly by rat tail plethysmograph.

High-throughput sequencing

Bacterial genomic DNA was extracted from colonic content using the standard Power Soil Kit protocol. For Roche 454 pyrosequencing (454 Life Sciences Roche, Branford, PA, USA), the V4–V5 regions of the 16S rRNA gene were PCR-amplified using bar-coded universal primers containing linker sequences.[25] The V4–V5 regions of the 16S rRNA gene were also PCR-amplified with primers containing linker sequences for Illumina MiSeq sequencing.[26]

16S rRNA gene sequencing analysis

Raw sequences obtained from 454 sequencing were quality-filtered by Mothur (http://www.mothur.org/) to obtain unique reads.[27] Sequences $\leqslant$200 bp or $\geqslant$1000 bp, as well as sequences containing any primer mismatches, barcode mismatches, ambiguous bases and homopolymer runs exceeding six bases were excluded. Raw sequences obtained from MiSeq sequencing were quality-filtered using QIIME.

All remaining sequences were assigned to operational taxonomic units (OTUs) with a 97% pairwise identity threshold, and then classified taxonomically using the Ribosomal Database Project (RDP) Classifier with a confidence threshold of 80%.[28] These taxonomies were used to construct summaries of the taxonomic distributions of OTUs, which could then be used to calculate the relative abundances of microbiota at different levels. Shannon and Simpson indices were calculated for α-diversity. Clinical indices were then tested for association to genera using Spearman rank correlation.

Cell culture and treatment

The normal rat kidney proximal tubular epithelial cell line (NRK-52E) and normal rat kidney interstitial fibroblast line (NRK-49F) purchased from the China Center for Type Culture Collection were used to evaluate the therapeutic effects of ABA on TGF-β1 or β-catenin stimulation. NRK-49F and NRK-52E cells were cultured in DMEM-F12 with 10% fetal bovine serum (Gibco, Carlsbad, CA, USA) at 37°C with 5% CO_2. Recombinant human TGF-β1 (R&D Systems, Minneapolis, MN, USA) was used at 5 ng/mL and 2.5 ng/mL, respectively, to stimulate NRK-49F and NRK-52E cells, in the presence or absence of ABA (10 μM). Recombinant human angiotensin II protein (R&D systems) was used at 1.0 μM and 2.0 μM to respectively stimulate NRK-49F and NRK-52E cells in the presence or absence of ABA (10 μM).

Cell viability analysis by CCK-8 and toxicity

Cells (1×10^4) cultured in 96-well plates were treated with ABA (0, 2.5, 5.0, 10, 20, 40 μM) for 24 h. The CCK-8 kit (EnoGene, Nanjing, China) was used to assess cell viability according to the manufacturer's protocol. The absorbance at 450 nm was measured by a microplate reader (Thermo Scientific, New York, NY, USA). The cell viability corresponding to each concentration tested was analysed six times.

Knockdown of Smad3 by small-interfering RNA

Lipofectamine RNAiMAX (Invitrogen, New York, NY, USA) was used for small-interfering

RNA (siRNA)-knockdown of Smad3. At 60% confluence, NRK-49F cells were transfected with Smad3 or control siRNA according to the manufacturer's protocols. Cells were treated as indicated 48 h after transfection.

qRT-PCR

Total RNA isolation and qRT-PCR were carried out according to previously described procedures.[29] The primers used in this study are presented in Supplemental Table S1.

Western blot analysis

Protein expression was analysed by Western blot analysis as previously described.[29] Blots were developed with ECL reagent and protein levels were normalised against α-tubulin expression.

Immunohistochemical and immunofluorescence staining

Immunohistochemical staining of kidney tissues was performed as previously described.[29,30] Immunofluorescent staining of kidney tissues or cells was carried out as previously described.[23] The tissue or cell sections were fixed with 4% paraformaldehyde. After blocking with normal goat serum, sections were stained with primary antibodies. After incubation with Alexa Fluor® 488- or 594-conjugated secondary antibodies, sections were visualised using a laser-scanning confocal microscope and analysed using FV10-ASW 4.0 VIEW.

Smad3-dependent promoter assay

NRK-52E cells were transfected with a Smad3 responsive promoter p(GAGA)12-luc as previously described.[23] Lipofectamine 3000 was used as a transfection reagent according to the manufacturer's instructions. After transfection, NRK-52E cells were treated with TGF-β1 and ABA. Luciferase activity was analysed by the Luciferase Reporter Gene Assay kit (Roche, Mannheim, Germany) according to the manufacturer's instructions, and was normalised in relation to protein concentration.

Co-immunoprecipitation

The precipitated complexes were analysed by Western blot analysis as previously described.[31]

Statistical analysis

The results are represented as mean ± standard deviation (SD). Statistical analyses were performed with GraphPad Prism software v 6.0 (San Diego, CA, USA). A two-tailed unpaired Student's *t* test was used to compare two groups, and statistically significant differences ($p < 0.05$) among more than two groups were detected using one-way analysis of variance (ANOVA) followed by Dunnett's *post hoc* tests (assuming equal variance).

Results

The chemical structure and toxicity of ABA

ABA was extracted and isolated from *A rhizoma* and identified using previously described procedures.[23] Its chemical structure is shown in Figure 1a. To evaluate the potential toxicity of ABA, NRK-52E cells were incubated in media containing different concentrations of ABA. Cell viability was analysed by the CCK-8 assay. ABA did not affect cell viability or proliferation at a dose of 2.5–40 μM (Supplemental Figure 1).

ABA treatment changes the dysbiosis of the gut microbiome

Gut microbiomes were characterised using Illumina Miseq sequencing with colonic lumenal content samples. Small decreases in gut microbiome diversity and richness were observed in the different groups (Figure 1b). A significant difference in β-diversity was observed based on sparse partial least squares-discriminate analysis (sPLS-DA) but not principal component analysis (PCA) (Figure 1c). At the phylum level, Firmicutes (67.1%) and Bacteroidetes (26.3%) dominated the gut microbiota of the three groups but in different ratios (Figure 1d). The main discriminant genera, *Lactobacillus*, *Allobaculum*, *Lactococcus*, *Clostridium_XlVa*, *Bacillus*, *Prevotella*, *Eubacterium* and *Ruminococcus*, were at higher abundance in the three groups (Figure 1e). Figure 1f illustrates the microbial taxa (phylum, class, order and family) that changed significantly in the colon of NX rats.

At the genus level, 12 genera exhibited significant differences in abundance in NX rats compared with the sham rats (Figure 1g). Of these, changes in 10 genera were reversed by ABA treatment (Figure 1g). Interestingly, enrichment of *Allobaculum*,

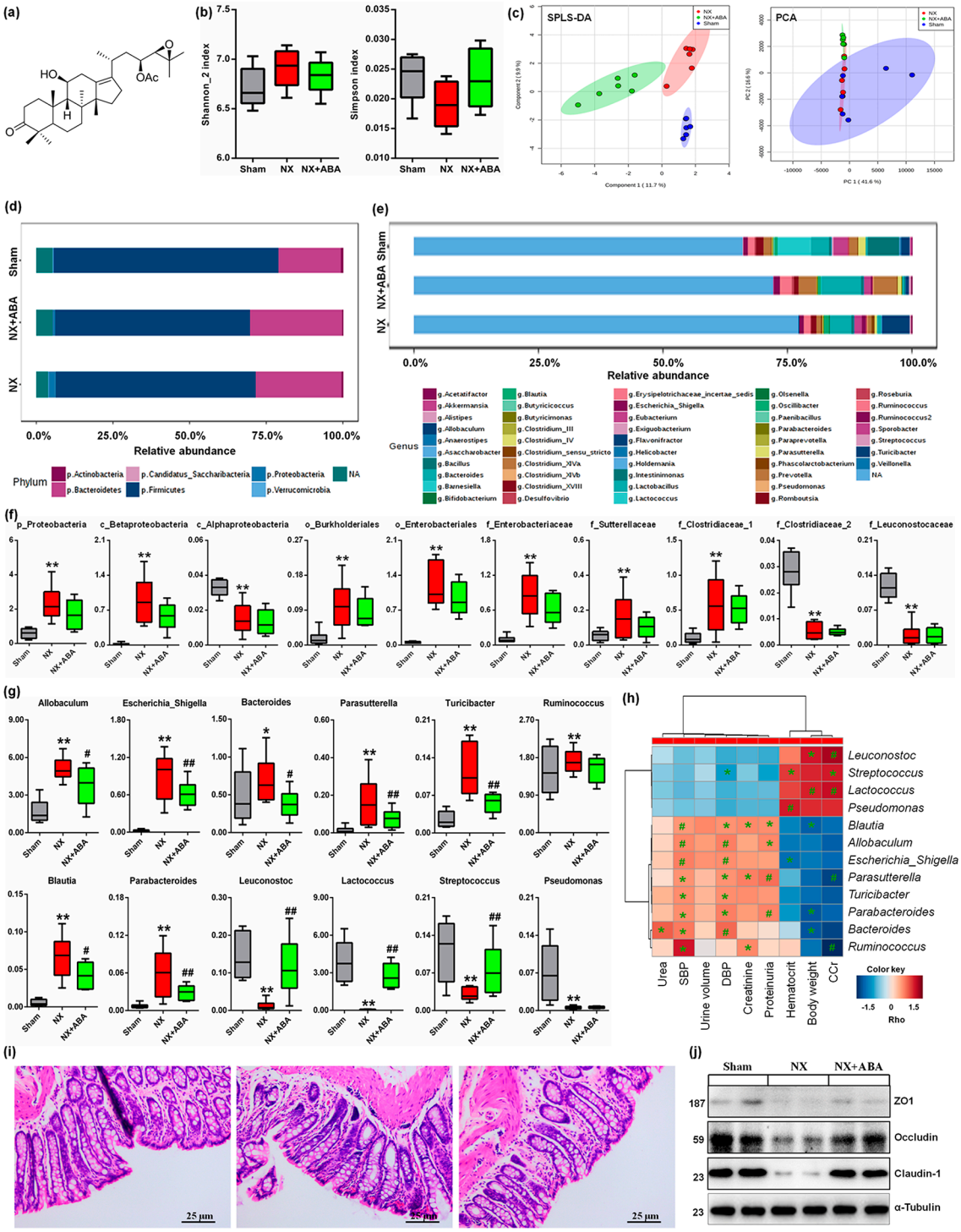

Figure 1. ABA treatment changes the dysbiosis of gut microbiome. (a) The chemical structure of ABA. (b) Shannon_2 and Simpson of α-diversity index of colonic content 16S rDNA sequencing data in the different groups. (c) The sPLS-DA and PCA of 16S rDNA profiling (OTUs level) of colonic lumenal content in the different groups. (d) Taxonomic distributions of bacteria from colonic lumenal content 16S rDNA sequencing data at the phylum (top 10) levels in the different groups. (e) Taxonomic distributions of bacteria from colonic lumenal content 16S rDNA sequencing data at the genus (top 30) levels in the different groups. (f) Comparison

(Continued)

Figure 1. *(Continued)*

of relative abundance of significantly bacterial taxa, including phylum, class, order and family levels in the different groups. *$p < 0.05$, **$p < 0.01$ *versus* sham rats ($n = 6$). (g) Comparison of relative abundance of significantly genera in the different groups. *$p < 0.05$, **$p < 0.01$ *versus* sham rats ($n = 6$). #$p < 0.05$, ##$p < 0.01$ *versus* NX rats ($n = 6$). (h) Spearman's rank correlation between 12 most differential genera and clinical indices. The results are presented as a heatmap using Ward clustering analysis. Rho in the colour key represents Spearman rank correlation coefficient. *$p < 0.05$, #$p < 0.01$ denote statistical significance between bacterial genera and clinical indices. (i) H&E staining of colon tissues in the different groups. (j) The protein expression of ZO1, occludin and claudin-1 in colon ($n = 6$).
ABA, alisol B 23-acetate; H&E, haematoxylin and eosin; NX, 5/6 nephrectomised; OTU, operational taxonomic units; PCA, principal component analysis; sPLS-DA, sparse partial least squares-discriminate analysis.

Escherichia_Shigella, *Bacteroides*, *Parasutterella* and *Blautia* and the depletion of *Lactococcus*, and *Leuconostoc* has been previously reported in hypertensive rats and patients,[32–34] which coincides with our findings in NX-induced hypertensive rats. Spearman correlation analysis showed that systolic blood pressure (SBP) and diastolic blood pressure (DBP) correlated with the enrichment of genera in the three groups, followed by proteinuria and CCr (Figure 1h). Histological analysis revealed that ABA treatment restored intestinal epithelial tight junctions and reduced intestinal permeability (Figure 1i), which is consistent with upregulation of ZO1, occludin, and claudin-1 protein expression following ABA treatment (Figure 1j). Taken together, these findings suggest that ABA protects against renal fibrosis in part by re-establishing dysbiosis of the gut microbiome and regulating blood pressure.

ABA ameliorates hypertension and inhibits RAS activation

To investigate whether ABA protects against renal fibrosis by improving hypertension, we next examined the effect of ABA on blood pressure and RAS in NX rats. Elevation of SBP was accompanied by activation of RAS at 12 weeks after NX. However, ABA treatment reversed hypertension in NX rats (Table 1). Upregulation of RAS components including AGT, angiotensin-converting-enzyme (ACE) and AT1R was observed in NX rats (Figure 2a–d). ABA treatment reversed the upregulation of RAS in NX and UUO rats. (Figure 2c, d). Incubation with TGF-β1 induced significant activation of all RAS components in cultured NRK-52E and NRK-49F cells (Figure 2e, f). Addition of ABA to the culture medium significantly inhibited the expression of RAS components . Similar results were observed in ANG-stimulated NRK-52E and NRK-49F cells (Supplemental Figure 2). These data suggest that ABA can ameliorate hypertension *in vivo* and simultaneously inhibit multiple RAS components *in vivo* and *in vitro*.

ABA administration improves renal function and inhibits TIF

ABA treatment at dosages of 5, 10 and 20 mg/kg significantly reduced serum creatinine and urea levels in CKD rats, with the most effective dose being 10 mg/kg (Table 1). Therefore, 10 mg/kg of ABA was selected for subsequent experiments. ABA treatment significantly attenuated the upregulation of alpha smooth muscle actin (α-SMA), collagen I, fibronectin and vimentin, and downregulation of E-cadherin in NX rats at both the mRNA and protein levels (Figure 3a, b). Periodic acid–Schiff (PAS) and Masson trichrome staining showed marked interstitial inflammation and fibrosis in placebo-treated NX rats (Figure 3b). ABA treatment significantly inhibited inflammatory cell infiltration and TIF. Furthermore, ABA treatment significantly inhibited the expression of fibrotic hallmarks in UUO rats at both mRNA and protein levels (Figure 3c–e). Taken together, these results demonstrate that ABA treatment not only prevents TIF, but also attenuates established TIF.

ABA suppresses Smad3 phosphorylation and preserves Smad7 expression in rat models of NX and UUO

To elucidate the mechanism through which ABA exerts its anti-TIF effects, both UUO and NX rat models were used. Smad7 is an inhibitory Smad that negatively regulates Smad2/3 activation by targeting TGFβRI and Smad2/3 for degradation *via* the ubiquitin proteasome degradation

Table 1. General parameters in the NX rats after the different dosese of ABA treatment.

Group	Sham	NX	NX+ABA (5 mg/kg)	NX+ABA (10 mg/kg)	NX+ABA (20 mg/kg)
Body weight (g)	404.7 ± 13.8	385.6 ± 17.7**	394.1 ± 15.3#	403.5 ± 14.7#	403.5 ± 14.7#
SBP (mmHg)	124.8 ± 7.2	169.1 ± 12.1**	157.1 ± 10.1#	145.9 ± 12.8##	143.9 ± 13.4##
Serum creatinine (μmol/L)	46.2 ± 4.8	97.3 ± 12.5**	82.9 ± 9.6#	73.9 ± 11.1##	70.9 ± 13.4##
Urea (mmol/L)	8.6 ± 1.8	18.9 ± 4.5**	14.7 ± 3.2#	12.7 ± 3.6##	10.7 ± 4.2##
Creatinine clearance (mL/min)	1.36 ± 0.45	0.81 ± 0.25**	1.11 ± 0.26#	1.28 ± 0.34##	1.32 ± 0.31##
Urine protein (mg/24 h)	8.5 ± 2.6	120.9 ± 15.9**	101.4 ± 13.9#	75.4 ± 11.7##	69.9 ± 15.1##

**$p < 0.01$ compared with the control group; #$p < 0.05$, ##$p < 0.01$ compared with the NX group.
ABA, alisol B 23-acetate; NX, 5/6 nephrectomised; SBP, systolic blood pressure.

machinery.[35] p-Smad2, Smad2, p-Smad3, Smad3 and Smad4 were significantly upregulated and Smad7 was significantly downregulated in the kidney of UUO rats compared with sham-operated rats. ABA treatment significantly suppressed the expression of p-Smad3 and preserved Smad7, but did not alter expression levels of other Smad proteins (Figure 4a, b). Additionally, ABA treatment did not affect the expression of ERK1/2, p38 and PI3K proteins or their phosphorylated forms (Figure 4c, d). Similarly, treatment with ABA significantly suppressed p-Smad3 and retained Smad7 but did not affect p-Samd2, p-ERK1/2, p-p38, or p-PI3K expression in the kidney of NX rats (Figure 4e, f). In addition, immunohistochemical analysis revealed that ABA treatment inhibits nuclear translocation of p-Smad3 (Figure 4g). Taken together, these data demonstrate that ABA treatment impedes Smad3 phosphorylation and preserves Smad7 expression levels in the TGF-β/Smad signaling pathway.

ABA attenuates EMT, inhibits Smad3 phosphorylation and preserves Smad7 expression in cultured renal epithelial cells

To explore the mechanisms underlying the anti-TIF effects of ABA observed in rat CKD models, we further investigated the effect of ABA on TGF-β1-induced EMT in NRK-52E cells. ABA treatment inhibited the expression of α-SMA, collagen I, fibronectin, and vimentin, the hallmarks of EMT in cultured NRK-52E cells (Figure 5a, b). Immunofluorescence analysis also indicated that ABA attenuates TGF-β1-induced upregulation of α-SMA (Figure 5c). ABA treatment suppressed p-Smad3 and preserved Smad7 expression but did not affect p-Samd2 and Smad4 expression in NRK-52E cells exposed to TGF-β1 (Figure 5d, e). Moreover, ABA treatment did not affect the phosphorylation of ERK1/2, p38 and PI3K in TGF-β1-stimulated NRK-52E cells (Figure 5f, g). By utilizing a luciferase reporter system containing the promoter region of the human collagen I gene, we found that ABA treatment ameliorated TGF-β1-induced Smad3-dependent collagen I promoter activity (Figure 5h). Immunofluorescence analysis also revealed that ABA suppresses p-Smad3 expression (Figure 5i). Taken together, these data demonstrate that ABA treatment suppresses Smad3 phosphorylation and preserves Smad7 in TGF-β1-stimulated NRK-52E cells, supporting the findings of our *in vivo* experiments.

ABA improves profibrogenic factor expression by a Smad3-dependent mechanism

We next examined whether p-Smad3 and Smad7 are the main therapeutic targets of ABA. Given that TGFβRII phosphorylates TGFβRI, which binds to and phosphorylates Smad2 and Smad3 under pathological conditions, we first examined the inhibitory effect of knocking down Smad3 in NRK-52E cells. As shown in Figure 6a, Smad3 expression was significantly downregulated by Smad3-specific siRNA. Although ABA treatment did not affect the process of RNAi or Smad3 expression (Figure 6b), knockdown of Smad3 significantly weakened the

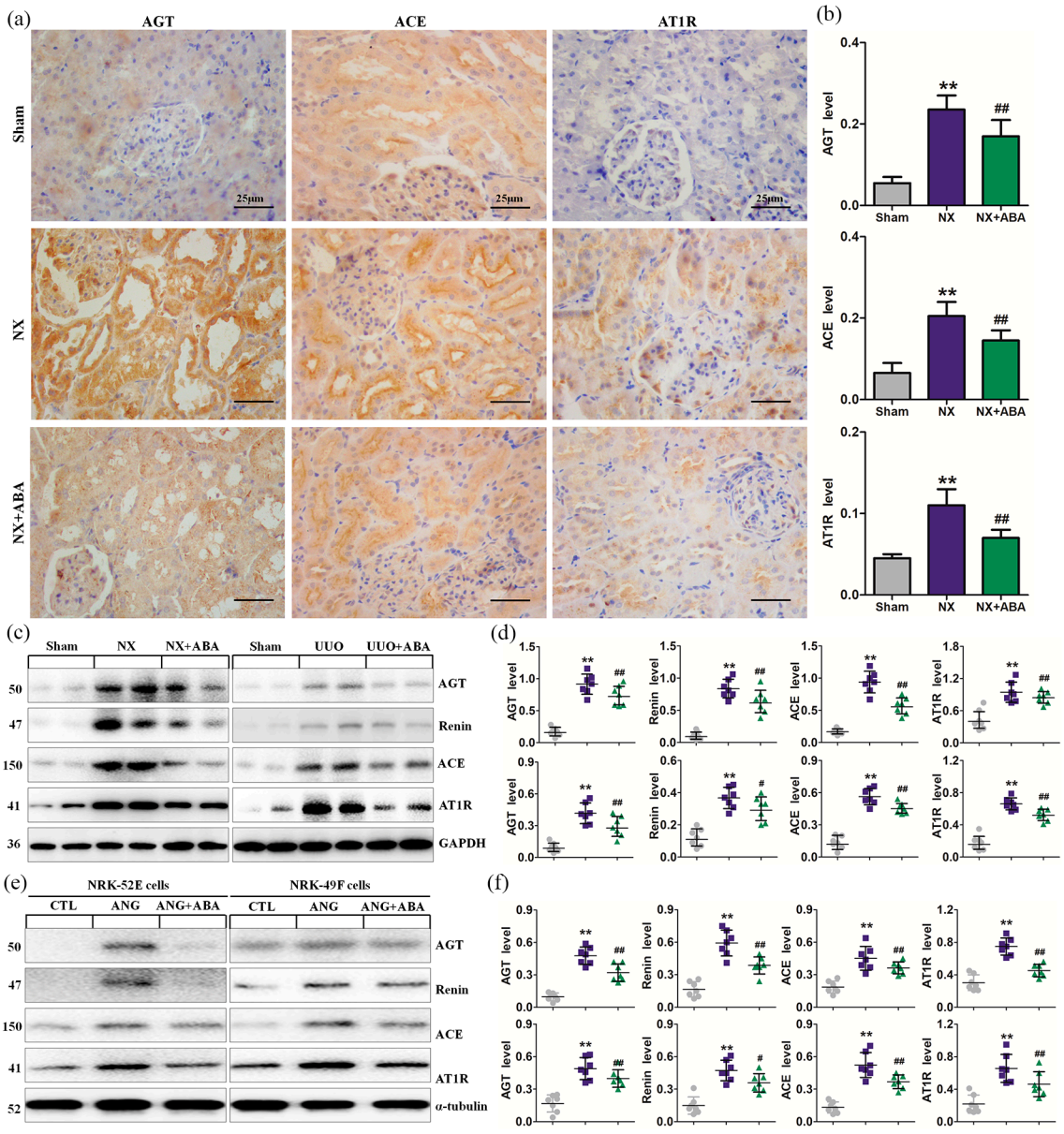

Figure 2. ABA treatment inhibits the activation of RAS. (a) Representative micrographs of AGT, ACE and AT1R. (b) Quantitative analysis of AGT, ACE and AT1R in the different groups of NX rats. (c) Protein expression of AGT, renin, ACE and AT1R in the different groups of NX rats. (d) Quantitative analyses of protein expression of AGT, renin, ACE and AT1R in the different groups. (e) Protein expression of AGT, renin, ACE and AT1R in the different groups of NRK-52E and NRK-49F cells. (f) Quantitative analyses of protein expression of AGT, renin, ACE and AT1R in the different groups of NRK-52E and NRK-49F cells. $^{*}p < 0.05$; $^{**}p < 0.01$ *versus* sham or CTL group. $^{\#}p < 0.05$; $^{\#\#}p < 0.01$ *versus* NX or UUO or ANG group ($n = 7$).

ABA, alisol B 23-acetate; ACE, angiotensin-converting-enzyme; AGT, angiotensinogen; ANG, angiotensin; AT1R, angiotensin II type 1 receptor; CTL, control; NX, 5/6 nephrectomised; RAS, renin–angiotensin system; UUO, unilateral ureteral obstructed.

inhibitory effect of ABA on the expression of profibrogenic proteins (Figure 6c, d). We then conducted Co-IP analysis to determine the effect of ABA treatment on the TGFβRI-Smad3 interaction. TGFβRI was clearly observed to bind Smad2 and Smad3 in the remnant kidney tissues of NX rats. ABA treatment significantly reduced the Smad3-TGFβRI interaction but did not affect the interaction between Smad2 and TGFβRI (Figure 6e, f). These data indicate

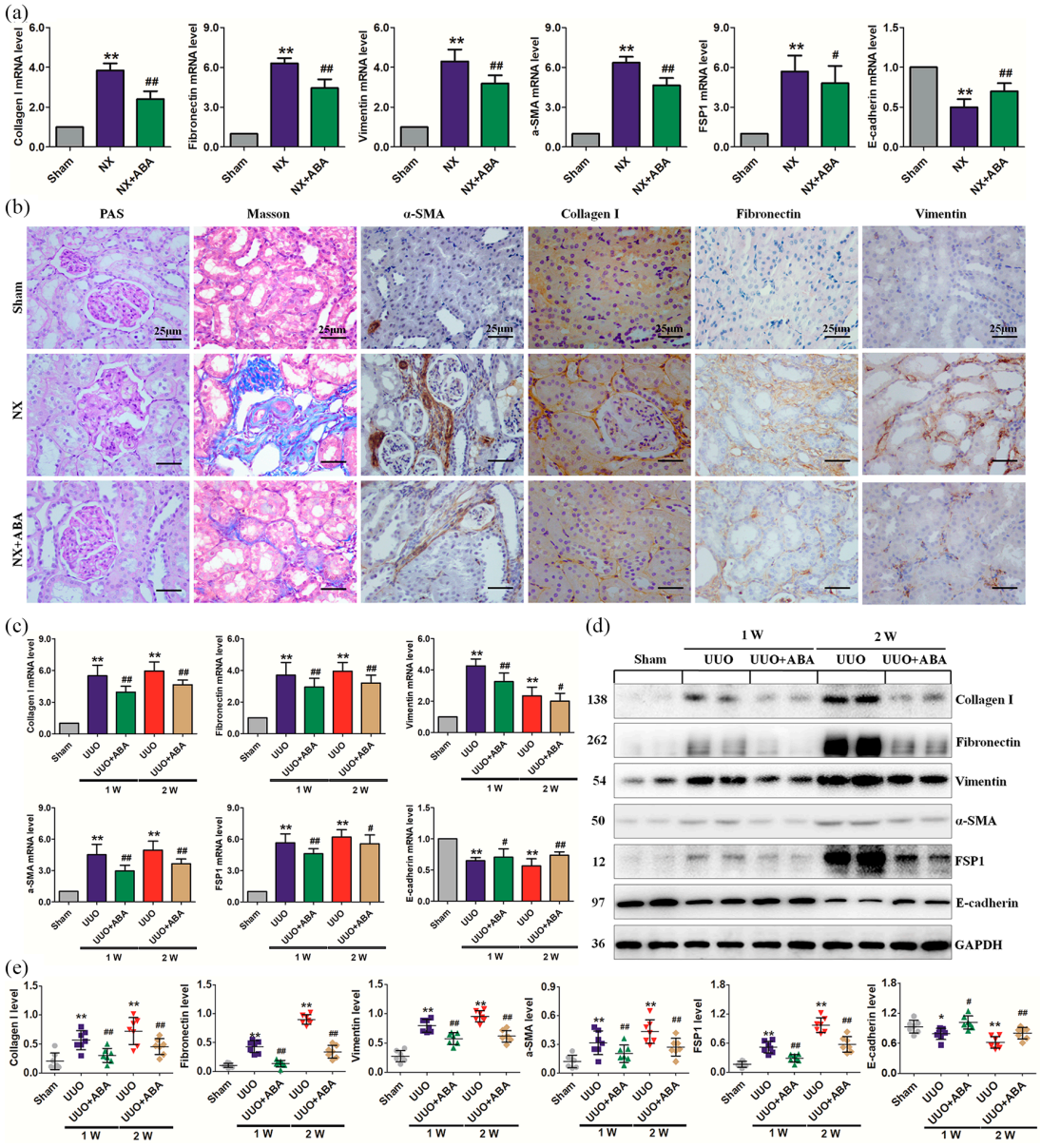

Figure 3. ABA attenuates renal dysfunction and fibrosis in UUO and NX models. (a) The mRNA expression of collagen I, fibronectin, vimentin, α-SMA, FSP1 and E-cadherin in the different groups of NX rats. (b) Representative micrographs of PAS and Masson's trichrome stainings and immunohistochemical staining including α-SMA, collagen I, fibronectin and vimentin in the different groups of NX rats. (c) mRNA expression of collagen I, fibronectin, vimentin, α-SMA, FSP1 and E-cadherin in the different groups of UUO rats. (d) Protein expression of collagen I, fibronectin, vimentin, α-SMA and FSP1 in the different groups of UUO rats at weeks 1 and 2. (e) Quantitative analyses of protein expression of collagen I, fibronectin, vimentin, α-SMA and FSP1 in the different groups of UUO rats at weeks 1 and 2. $^{*}p<0.05$; $^{**}p<0.01$ *versus* sham group. $^{\#}p<0.05$; $^{\#\#}p<0.01$ *versus* NX or UUO group ($n=7$).
ABA, alisol B 23-acetate; α-SMA, alpha smooth muscle actin; FSP1, fibroblast-specific protein 1; NX, 5/6 nephrectomised; PAS, periodic acid–Schiff; UUO, unilateral ureteral obstructed.

that ABA treatment selectively inhibits the Smad3–TGFβRI interaction.

Smad7 acts as an adaptor protein to recruit E3 ubiquitin ligases such as Smurf2 to the TGFβR complex to promote its degradation through proteasomal-ubiquitin degradation pathways.[35] Degradation of Smad7 also leads to activation of Smad2 and Smad3, thereby aggravating renal fibrosis.[35] As such, we further examined the effect

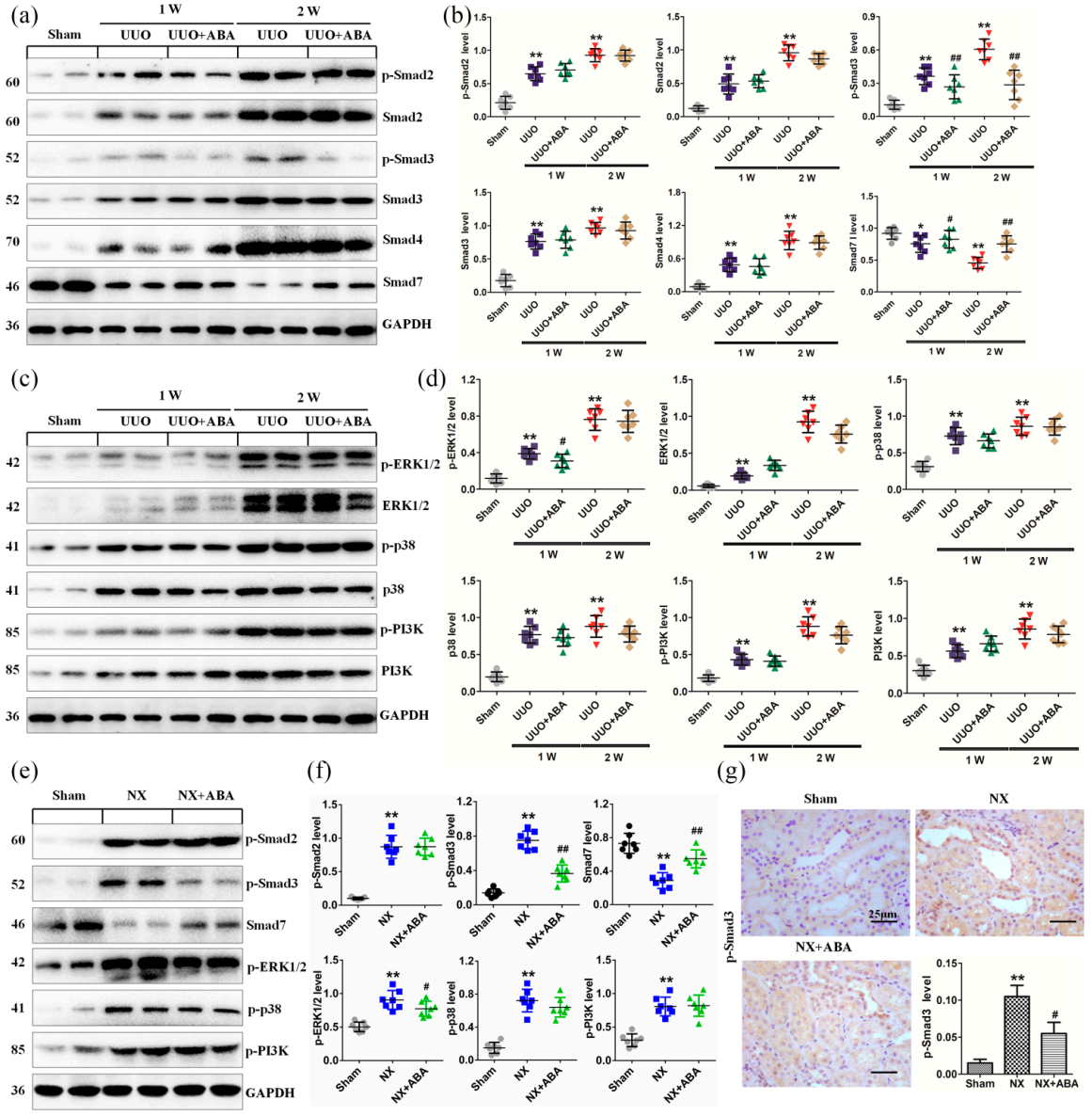

Figure 4. ABA mitigates renal fibrosis by inhibiting Smad3 phosphorylation and preserving Smad7 expression. (a) Protein expression of TGF-β1, p-Smad2, Smad2, p-Smad3, Smad3, Smad4 and Smad7 in the different groups of UUO rats at weeks 1 and 2. (b) Quantitative analyses of protein expression of TGF-β1, p-Smad2, Smad2, p-Smad3, Smad3, Smad4 and Smad7 in the different groups of UUO rats at weeks 1 and 2. (c) Protein expression of TGF-β1, p-ERK1/2, ERK1/2, p-p38, p38, p-PI3K and PI3K in the different groups of UUO rats at weeks 1 and 2. (d) Quantitative analyses of protein expression of TGF-β1, p-ERK1/2, ERK1/2, p-p38, p38, p-PI3K and PI3K in the different groups of UUO rats at weeks 1 and 2. (e) Protein expression of p-Smad2, p-Smad3, p-ERK1/2, p-p38, p-PI3K and Smad7 in the different groups of NX rats. (f) Quantitative analyses of protein expression of p-Smad2, p-Smad3, p-ERK1/2, p-p38, p-PI3K and Smad7 in the different groups of NX rats. (g) Representative micrographs of p-Smad3 in the different groups of NX rats. *$p < 0.05$; **$p < 0.01$ *versus* sham group. #$p < 0.05$; ##$p < 0.01$ *versus* NX or UUO group (n = 7).

ABA, alisol B 23-acetate; NX, 5/6 nephrectomised; PI3K, phosphatidylinositol 3-kinase; p-PI3K, phosphorylated PI3K; TGF-β1, transforming growth factor-β1; UUO, unilateral ureteral obstructed.

of ABA treatment on the interactions between TGFβRI and Smurf2, TGFβRI and Smad7, and Smurf2 and Smad7, and found that ABA treatment enhanced these interactions (Figure 6g, h).

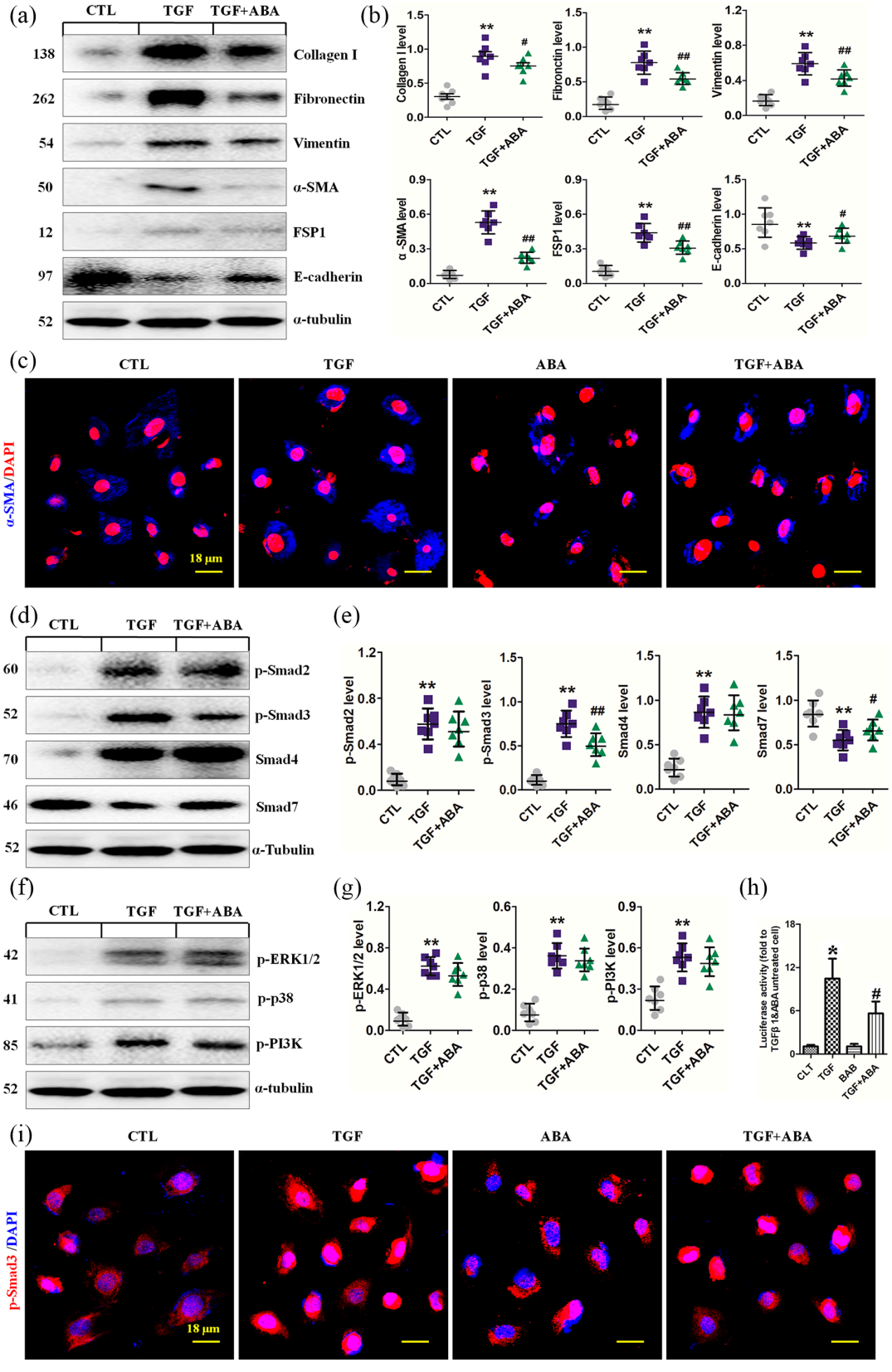

Figure 5. *(Continued)*

Figure 5. ABA selectively suppresses Smad3 phosphorylation and preserves Smad7 expression in TGF-β1-induced NRK-52E cells. (a) Protein expression of collagen I, fibronectin, vimentin, α-SMA, FSP1 and E-cadherin in the different groups of TGF-β1-induced NRK-52E cells. (b) Quantitative analyses of protein expression of collagen I, fibronectin, vimentin, α-SMA, FSP1 and E-cadherin in the different groups of TGF-β1-induced NRK-52E cells. (c) Immunofluorescence staining of TGF-β1 upregulates α-SMA (blue) and p-Smad3 (red) in the different groups of TGF-β1-induced NRK-52E cells. (d) Protein expression of TGF-β1, p-Smad2, p-Smad3, Smad4, and Smad7 in the different groups of the TGF-β1-induced NRK-52E cells. (e) Quantitative analyses of protein expression of TGF-β1, p-Smad2, p-Smad3, Smad4 and Smad7 in the different groups of TGF-β1-induced NRK-52E cells. (f) Protein expression of TGF-β1, p-ERK1/2, p-p38, p-PI3K in the different groups of TGF-β1-induced NRK-52E cells. (g) Quantitative analyses of protein expression of TGF-β1, p-ERK1/2, p-p38, p-PI3K in the different groups of TGF-β1-induced NRK-52E cells. (h) Relative luciferase activity in the different groups of the TGF-β1-induced NRK-52E cells. (i) Representative immunofluorescent staining of p-Smad3 expression in the different groups of TGF-β1-induced NRK-52E cells. $^{*}p < 0.05$; $^{**}p < 0.01$ *versus* CTL group. $^{\#}p < 0.05$; $^{\#\#}p < 0.01$ *versus* TGF group ($n = 7$).
ABA, alisol B 23-acetate; α-SMA, alpha smooth muscle actin; FSP1, fibroblast-specific protein 1; p-PI3K, phosphorylated phosphatidylinositol 3-kinase; TGF, transforming growth factor; TGF-β1, transforming growth factor-β1.

Moreover, ABA treatment enhanced the interaction between TGFβRI and Smurf2 or Smad7 and the interaction between Smurf2 and Smad7 to accelerate Smad3 degradation.

Collectively, these data suggest that ABA treatment may inhibit the TGF-β/Smad3 pathway by blocking the Smad3-TGFβRI interaction and thus Smad7 degradation.

ABA promotes apoptosis of renal fibroblasts and suppresses the Wnt/β-catenin signaling pathway

TIF is the consequence of renal fibroblast activation and proliferation, and suppression of these processes attenuates renal fibrosis. As such, we also explored the effects of ABA treatment on the death of renal interstitial fibroblasts (NRK-49F) in the absence or presence of TGF-β1. Exposure of NRK-49F cells to ABA resulted in the upregulation of several pro-apoptotic proteins, including mitochondrial Bcl-2, Bax, Cyto-C, cleaved caspase-9 and cleaved caspase-3, and downregulation of the major anti-apoptotic protein Bcl-2 in both the absence and presence of TGF-β1 stimulation. This suggests that ABA has proapoptotic effects in NRK-49F cells (Figure 7a, b).

Wnt/β-catenin signaling is a conserved developmental signaling cascade that plays an important role in cell survival.[36] We thus examined the effects of ABA treatment on the activation of this pathway. TGF-β1 stimulation induced the expression of Wnt1, Wnt2, Wnt3, Wnt3a, Wnt7a and Wnt8a mRNAs in NRK-49F cells, and ABA treatment inhibited the induction of these proteins. (Supplemental Figure 3). ABA treatment also mitigated Wnt1, active β-catenin and β-catenin expression, whereas it enhanced p-β-catenin expression in TGF-β1-treated NRK-52E cells (Figure 7c, d). In addition, immunofluorescence analysis indicated that ABA inhibited upregulation of β-catenin expression in TGF-β1-treated NRK-52E cells (Figure 7e).

Discussion

In this study, we first demonstrated that ABA treatment protected against TIF, in part by re-establishing dysbiosis of the gut microbiome and regulating blood pressure (Figure 8). Interestingly, the enrichment or depletion of 12 genera were associated with hypertension, which coincides with results from previous studies.[32,34] ABA treatment restored intestinal epithelial tight junctions and reduced intestinal permeability, which are consistent with ABA-mediated upregulation of ZO1, occludin and claudin-1 protein expression. We found that ABA treatment simultaneously inhibited multiple intrarenal RAS components and inhibits the TGF-β/Smad signaling pathway in both *in vivo* and *in vitro* settings. This suggests that ABA might inhibit hypertension and renal fibrosis by suppressing the expression of intrarenal RAS components and profibrotic signaling pathways. ABA is also effective in suppressing Wnt/β-catenin and mitochondrial-associated caspase signaling pathways in TGF-β1-induced cells. These data indicate that ABA is a potent inhibitor of renal hypertension and fibrosis, and suggest that it is a potential drug candidate for CKD treatment.

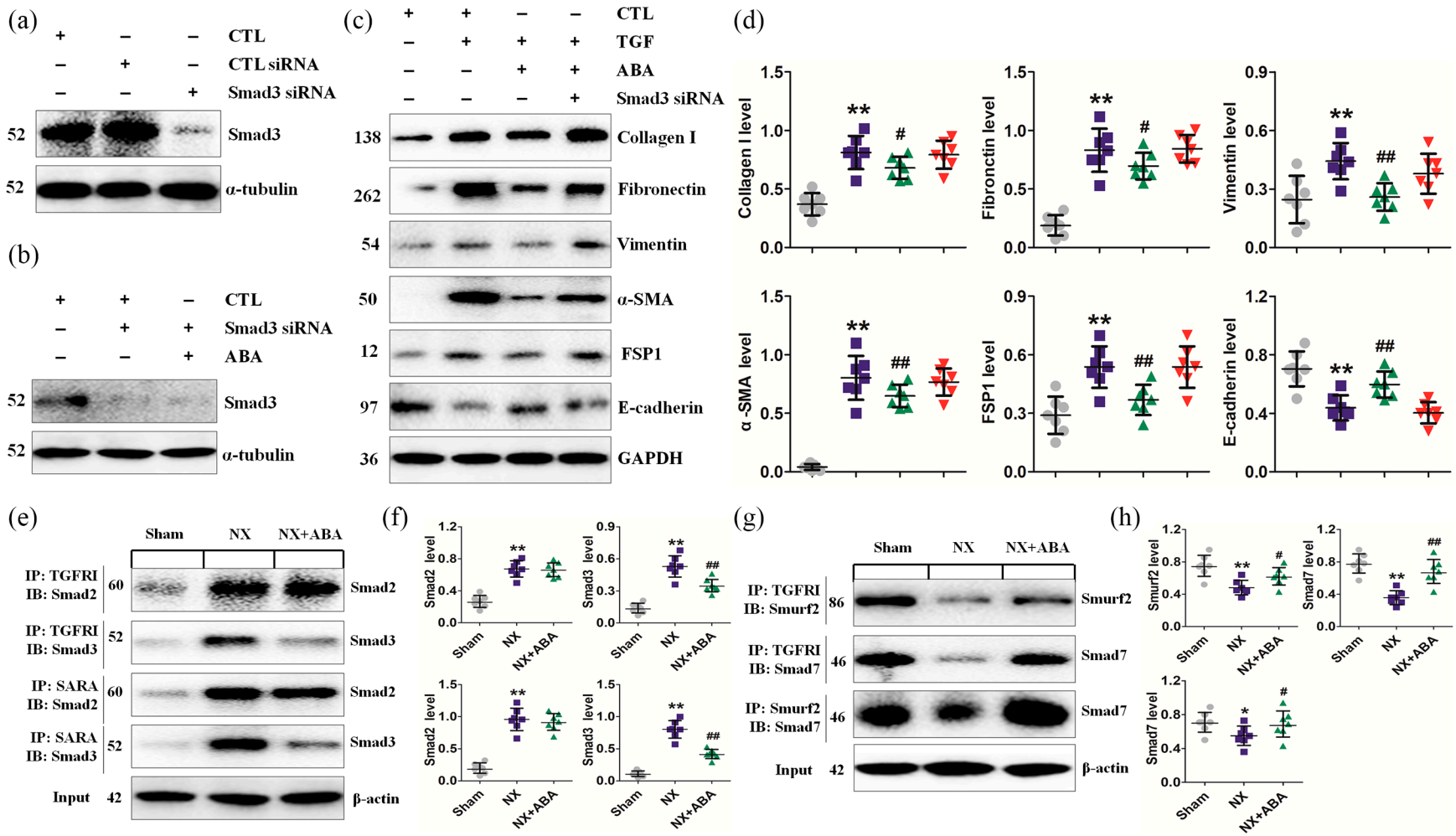

Figure 6. Smad3 and Smad7 are the main therapeutic targets of ABA to reduce fibrosis. (a) Protein expression of Smad3 in the NRK-52E cells induced by Smad3 siRNA. (b) After infection with Smad3 siRNA, protein expression of Smad3 was determined in NRK-52E cells treated with ABA. (c) Protein expression of collagen I, fibronectin, vimentin, α-SMA, FSP1 and E-cadherin in TGF-β1-induced NRK-52E cells treated by Smad3 siRNA and ABA. (d) Quantitative analyses of protein expression of collagen I, fibronectin, vimentin, α-SMA, FSP1 and E-cadherin in TGF-β1-induced NRK-52E cells treated by Smad3 siRNA and ABA. (e) Protein expression of Smad2 and Smad3 treated by CO-IP method in the different groups as indicated. (f) Quantitative analyses of protein expression of Smad2 and Smad3 treated by CO-IP method in the different groups as indicated. (g) Protein expression of Smad7 or Smurf2 treated by CO-IP method in the different groups as indicated. (h) Quantitative analyses of protein expression of Smad7 or Smurf2 treated by CO-IP method in the different groups as indicated. $^{*}p < 0.05$; $^{**}p < 0.01$ *versus* sham or CTL group. $^{\#}p < 0.05$; $^{\#\#}p < 0.01$ *versus* NX or TGF group ($n = 7$).

ABA, alisol B 23-acetate; α-SMA, alpha smooth muscle actin; CO-IP, co-immunoprecipitation; CTL, control; FSP1, fibroblast-specific protein 1; PI3K, phosphatidylinositol 3-kinase; p-PI3K, phosphorylated PI3K; siRNA, small interfering RNS; TGF, transforming growth factor; TGF-β1, transforming growth factor-β1.

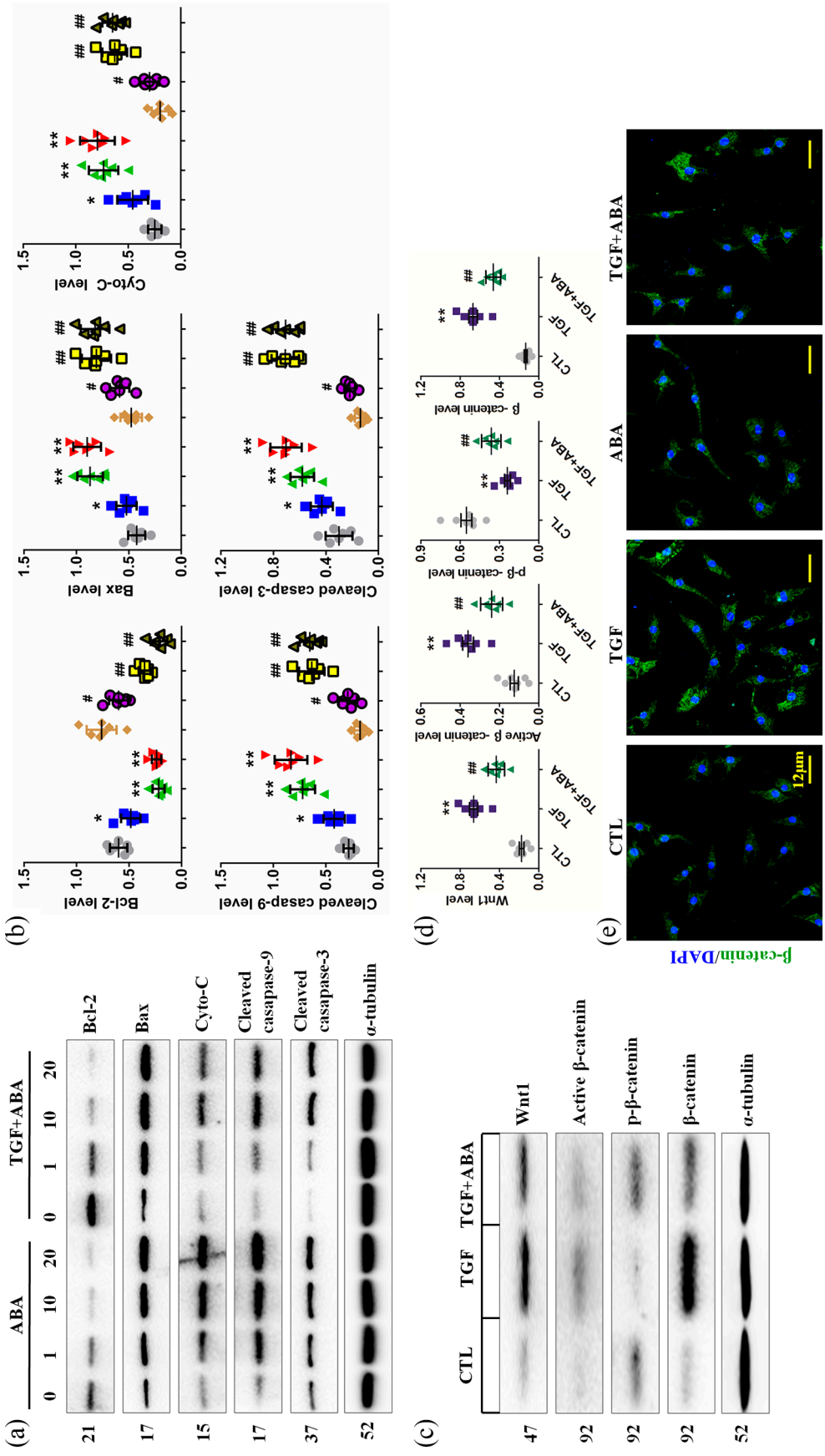

Figure 7. ABA contributes to the apoptosis of fibroblasts through regulating the Wnt/β-catenin pathway. (a) Protein expression of Bcl-2, Bax, Cyto-C, cleaved caspase-9 and cleaved caspase-3 in the different groups of TGF-β1-induced NRK-49F cells. (b) Quantitative analyses of protein expression of Bcl-2, Bax, Cyto-C, cleaved caspase-9 and cleaved caspase-3 in the different groups of TGF-β1-induced NRK-49F cells. (c) Protein expression of Wnt1, active β-catenin, p-β-catenin in the different groups of TGF-β1-induced NRK-49F cells. (d) Quantitative analyses of protein expression of Wnt1, active β-catenin and p-β-catenin in the different groups of the TGF-β1-induced NRK-49F cells. (e) Immunofluorescence staining of β-catenin (green) in the different groups of TGF-β1-induced NRK-49F cells.
$^{*}p < 0.05$; $^{**}p < 0.01$ *versus* CTL group. $^{\#}p < 0.05$; $^{\#\#}p < 0.01$ *versus* TGF group ($n = 7$).
ABA, alisol B 23-acetate; CAT, β-catenin; CTL, control; NX, 5/6 nephrectomised; TGF, transforming growth factor; TGF-β1, transforming growth factor-β1.

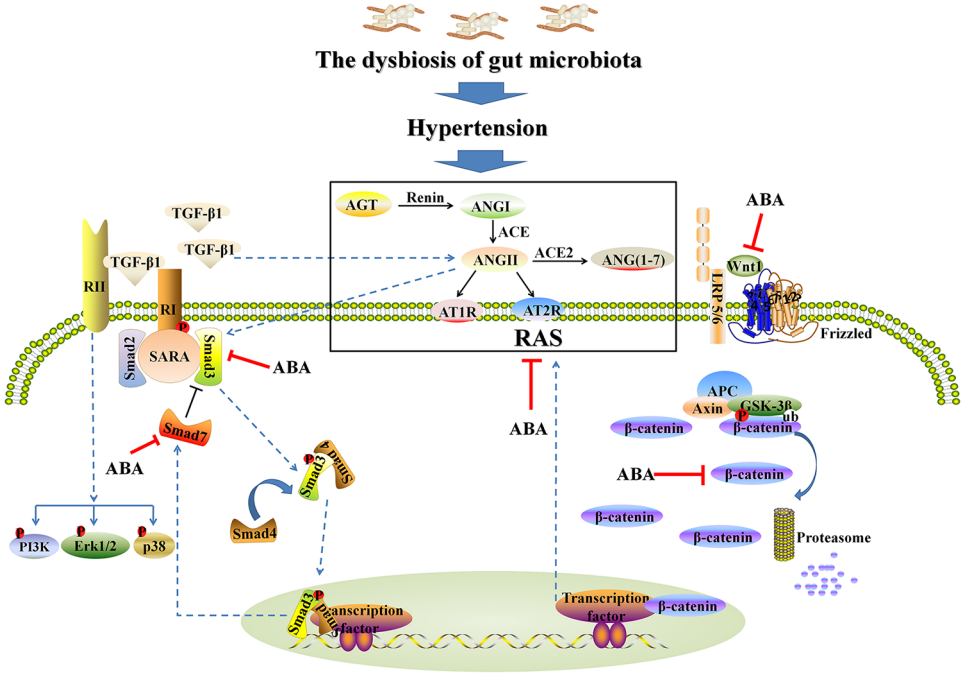

Figure 8. Schematic diagram depicting possible mechanisms involved in anti-hypertensive and renoprotective effects of ABA.

ABA, alisol B 23-acetate; ACE, angiotensin-converting-enzyme; AGT, angiotensinogen; ANGI, angiotensin I; ANGII, angiotensin II; APC, adenomatous polyposis coli; AT1R, angiotensin II type 1 receptor; AT2R, angiotensin II type 2 receptor; GSK3β, glycogen synthase kinase 3 beta; RAS, renin–angiotensin system; TGF-β1, transforming growth factor-β1.

Our current study demonstrates that hypertension is closely associated with dysbiosis of the gut microbiome in NX rats. Many excellent reviews have summarized the relationship between hypertension and dysbiosis of the gut microbiome in CKD.[37–40] Several seminal publications have highlighted that alterations in blood pressure are potentially linked to intestinal microorganisms.[32,41,42] Based on faecal metagenomic analysis, the most compelling evidence revealed that both pre-hypertensive and hypertensive subjects showed reduced microbial wealth and diversity, reduction in bacteria that are related to healthy status and prevalences of *Klebsiella* and *Prevotella* that are related to pathological conditions.[42,43] Similarly, another study demonstrated that hypertensive patients showed decreased diversity within faecal samples and found that opportunistic pathogenic taxa such as *Streptococcus* spp., *Klebsiella* spp. and *Parabacteroides merdae* were increased in hypertensive patients, while *Roseburia* spp. and *Faecalibacterium prausnitzii* were increased in healthy subjects.[44] In addition, fecal microbiome analysis showed that high salt intake enhanced the abundance of Firmicutes, Proteobacteria and *Prevotella* bacteria in healthy human volunteers, and predisposed mice to hypertension in response to a subpressor dose of angiotensin II.[45] Adoptive transfer of faecal material from high-salt-fed mice to germ-free mice predisposed them to increased hypertension.[45] Another study demonstrated that both a small cohort of hypertensive patients and spontaneously hypertensive rats showed a significant decrease in microbial richness, diversity and evenness as well as an increased Firmicutes/Bacteroidetes ratio in faecal samples.[41] In line with this, similar results were found in the chronic angiotensin II infusion rat model.[32] This latter study revealed that increased blood pressure was significantly associated with decreased tight junction proteins and increased intestinal permeability, and these gut pathological changes and hypertension were associated with alterations in microbial communities in spontaneously hypertensive rats.[32] Furthermore, this study also revealed activated gut-neuronal communication in hypertension originating from the paraventricular nucleus of the hypothalamus and increased sympathetic drive to the gut. In line with this, the ACEI captopril restored blood pressure that was related to reversal of gut pathology.[32]

Fibre consumption and drug treatment are used to improve dysbiosis of the gut microbiota and hypertension. A clinical trial was designed to assess whether minocycline treatment improved hypertensive effects in drug-resistant neurogenic hypertensive individuals. The results of this ongoing trial demonstrated that the gut microbiota of a subgroup of hypertensive patients was characterized by decreased microbial richness and diversity as compared with the gut microbiota of healthy subjects.[46] High fibre consumption independently modified gut microbiota populations and enhanced acetate-producing bacteria in mineralocorticoid excess-treated mice.[47] Both fibre and acetate supplementation improved gut dysbiosis as demonstrated by the Firmicutes/Bacteroidetes ratio and increased *Bacteroides acidifaciens* abundance. Two therapies significantly lowered SBP, DBP, cardiac fibrosis and left ventricular hypertrophy, whereas acetate supplementation showed similar effects and also reduced renal fibrosis.[47] Further transcriptome analyses showed that their protective effects were associated with downregulation of cardiac and renal *Egr1*, a master cardiovascular regulator implicated in inflammation, cardiac hypertrophy and cardiorenal fibrosis. This study has further elucidated the gene networks involved in circadian rhythmicity and inhibiting intrarenal RAS.[47] Chemically modified tetracycline-3 is a tetracycline derivative. Intracerebroventricular chemically modified tetracycline-3 ameliorated elevations in mean arterial pressure, and attenuated sympathetic activity and left ventricular hypertrophy in angiotensin II rats and spontaneously hypertensive rats.[48] Chemically modified tetracycline-3 reversed changes in certain gut microbial communities in faecal samples induced by angiotensin II and impeded pathological alterations in the gut wall.[48] In addition, oral minocycline ameliorated high blood pressure and rebalanced the dysbiotic gut microbiota by decreasing the Firmicutes/Bacteroidetes ratio in the chronic angiotensin II infusion rat model.[41]

The development of progressive kidney dysfunction, even after the apparent resolution of an injurious condition, is observed in many CKD cases. The model most frequently used to investigate the events that follow the loss of functioning renal tissue is the NX rat model.[49] A few publications have demonstrated dysbiosis of the gut microbiota in the NX model. For example, it has been reported that decreased amounts of stool and constipation in NX mice was related to an inhibited contraction response in ileum motility and a reduced relaxation response in distal colon motility.[50] Uremic toxins such as spermine inhibited the contraction response in ileum motility. NX disturbed the balance of the gut microbiota in mice. Antibiotic treatment improved ileum motility and constipation. The distal colon, but not the ileum, showed expression of inducible nitric oxide synthase, tumour necrosis factor-α and interleukin as well as macrophage infiltration in NX mice.[50] These findings revealed that NX altered gastrointestinal motility and led to constipation and colonic inflammation *via* dysbiosis of the gut microbiota, which demonstrated that CKD was associated with gastrointestinal dysregulation. Another study showed that impaired guts were accompanied with downregulation of colonic heat shock protein 70 and claudin-1 expression as well as upregulation of pore-forming claudin-2 expression and apoptosis in NX-induced CKD mice.[51] Orally administered lactobacilli partially retarded the CKD-induced impaired gut, restored colon epithelial claudin-1, heat shock protein 70 and claudin-2 expression and reduced apoptosis.[51] In addition, another study showed that NX rats exhibited lower abundances of *Firmicutes* and *Lactobacillus*, and lower haemoglobin and creatinine clearance and hypertension compared with sham rats.[52] The tryptophanase-possessing families *Verrucomicrobia*, *Enterobacteriaceae* and *Clostridiaceae* were decreased in NX rats. *Verrucomicrobia* was mostly represented by *Akkermansia muciniphila*, which has important roles in mucin degradation and gut barrier integrity.[52] Emodin is a naturally occurring anthraquinone present in *Rheum officinale*, which possesses multiple pharmacological activities such as diuretic, renoprotective, lipid-lowering, purgative and anti-inflammatory effects.[53–56] X Emodin via colonic irrigation reduced serum levels of urea and indoxyl sulphate, improved renal function and changed gut microbiota in NX-induced CKD rats.[57] Real-time qPCR analysis showed that emodin treatment restored dysbiosis of the gut microbiota in CKD. Emodin treatment inhibited the abundance of harmful bacteria such as *Clostridium* spp. that was positively correlated with both serum urea and indoxyl sulphate levels, but enhanced the abundance of beneficial bacteria including *Lactobacillus* spp. that was negatively correlated with serum urea levels.[57] Thus, emodin therapy induces changes in the gut microbiota that are

associated with reducing uremic toxins and mitigating renal injury. Taken together, these studies revealed that hypertension was associated with dysbiosis of the gut microbiota, associated gut barrier disruption and aberrant mucosal immunity in both animals and humans with CKD. Targeting the gut microbiota might provide novel therapeutic opportunities for CKD and renal fibrosis. Dietary intervention using probiotics, antibiotics, faecal transplant and combination pharmacotherapy might be an innovative nutritional therapeutic strategy for hypertension and CKD treatments by correcting dysbiosis of the gut microbiota. Therefore, our current findings demonstrate that ABA treatment of renal fibrosis was associated with attenuating hypertension and restoration of dysbiosis in the gut microbiome. ABA treatment could improve hypertension, further inhibit RAS and normalize aberrant gut microbiota through attenuated renal fibrosis.

Activation of the TGF-β/Smad signaling pathway plays a critical role in TIF. It is well established that binding of TGF-β1 to TGFβRII can activate TGFβRI, resulting in the phosphorylation and nuclear translocation of Smad2/Smad3 and subsequent upregulation of profibrotic genes.[58] A growing body of literature suggests that a multitude of compounds isolated from natural products attenuate tissue fibrosis, including renal fibrosis, by targeting the regulation of the TGF-β/Smad signaling pathway.[15,16,35,59] Our study demonstrates that ABA treatment dramatically suppresses TGF-β1-induced Smad3 phosphorylation and preserves Smad7 expression in both cultured NRK-52E cells and NX and UUO rat models. ABA treatment also blocks nuclear translocation of the Smad complex and inhibits the expression of Smad-driven genes including collagen I, fibronectin and α-SMA. However, ABA treatment did not affect Smad2 phosphorylation or Smad4 expression. Furthermore, ABA treatment did not affect the activation of multiple Smad-independent pathways of the downstream of TGF-β receptor, including ERK1/2, p38 and PI3K. This suggests that ABA is a selective inhibitor of Smad3. Smad2, Smad3 and Smad7 were thought to be the major target of drug intervention in TGF-β/Smad signaling pathway.[35,60] For example, previous studies demonstrated that poricoic acid A, poricoic acid ZA, poricoic acid ZC, poricoic acid ZD, poricoic acid ZE, poricoic acid ZG and poricoic acid ZH isolated from *Poria cocos* selectively inhibited Smad3 phosphorylation by blocking the interaction between TGFβRI and Smad3, while they did not affect Smad2, p-Smad2, Smad3 and Smad7 expression.[61–64] Although the mechanism by which ABA inhibits Smad3 activation remains unclear, we find that ABA treatment inhibits TGFβRI expression and retains Smad7 expression in the kidney of two CKD rat models as well as in TGF-β1-stimulated NRK-52E cells, suggesting that ABA may suppress Smad3 activation through a mechanism involving interference in Smad3 recruitment to TGFβRI and preservation of Smad7 expression.

To verify the role of Smad3 in mediating the anti-fibrotic effect of ABA, we examined the effect of Smad3 downregulation on the anti-fibrotic effects of ABA in TGF-β1-stimulated NRK-52E cells. siRNA-mediated knockdown of Smad3 partially reduces the anti-fibrotic effects of ABA, and ABA selectively suppresses the interaction of Smad3 with TGFβRI. Co-IP data also indicates that ABA treatment enhances the interaction of TGFβRI, Smad7 and Smurf2. Since Smad7-mediates Smurf2 recruitment to the TGF-β receptor complex to promote TGF-β receptor degradation,[65] these findings suggest that ABA treatment impedes TIF through a mechanism associated with enhancing Smad7-mediated inhibition of the TGF-/Smad3 signaling pathways.

Previous studies have demonstrated that activation of the Wnt/β-catenin signaling pathway enhances the expression of RAS components and accelerates renal fibrosis.[7,66] Many natural products attenuate renal fibrosis by modulating the Wnt/β-catenin signaling pathway.[67] Our previous study demonstrated that ABA treatment could inhibit the expression of proteins downstream of Wnt/β-catenin including Snail1, matrix metalloproteinase-7, twist and fibroblast-specific protein 1, and retard profibrotic protein expression and podocyte injury in ANG-induced HK-2 cells and podocytes.[68] Our current study indicates that ABA mitigates the expression of Wnt1, β-catenin and active β-catenin, whereas it enhanced p-β-catenin expression in TGF-β1-treated NRK-52E cells. Thus, RAS is linked to the TGF-β/Smad and Wnt/β-catenin signaling pathways and the pathogenesis of TIF. It seems that a vicious cycle is formed, in which RAS provokes TIF by triggering the TGF-β/Smad and Wnt/β-catenin signaling pathways, whereas, by limiting renal blood flow, TIF elevates arterial blood pressure and activates RAS, which in turn amplifies TGF-β/Smad and

Wnt/β-catenin activation.[4] Although the role of intrarenal RAS activation in progressive CKD is well established, the underlying mechanisms by which RAS components are modified in CKD conditions were previously elusive but have been elucidated herein. In addition, our study shows that ABA attenuates renal fibrosis and further inhibits the expression of RAS components.

Our current study has several limitations. Although ABA impeded renal fibrosis by restoring dysbiosis of the gut microbiome, attenuating hypertension and suppressing RAS components, the findings should be further verified in spontaneously hypertensive rats. In addition, dysbiosis of the gut microbiota in CKD should be further verified in other animal models.

In summary, ABA ameliorated TIF by re-establishing dysbiosis of the gut microbiome, ameliorating hypertension, and inhibiting RAS components. ABA also attenuated TIF by inactivation of renal fibroblasts, inhibition of EMT, and induction of renal fibroblast apoptosis. Mechanistically, ABA could inhibit Smad3 activation through preservation of Smad7 expression and preventing TGFβRI and Smad3 binding. ABA also suppresses the Wnt/β-catenin signaling pathway that is involved in the activation and proliferation of renal fibroblasts. It will be interesting to develop ABA as an anti-fibrotic drug to treat CKD.

Conflict of interest statement

The authors declare that there is no conflict of interest.

Funding

This study was supported by the National Key Research and Development Project of China (grant number 2019YFC1709405) and National Natural Science Foundation of China (grant numbers 81603271 and 81673578). No funding bodies had any role in study design, data collection, and analysis, decision to publish, or preparation of the manuscript.

ORCID iD

Ying-Yong Zhao https://orcid.org/0000-0002-0239-7342

Supplemental material

Supplemental material for this article is available online.

References

1. Malhotra R, Nguyen HA, Benavente O, *et al.* Association between more intensive vs less intensive blood pressure lowering and risk of mortality in chronic kidney disease stages 3 to 5: a systematic review and meta-analysis. *JAMA Intern Med* 2017; 177: 1498–1505.
2. Ruiz-Hurtado G, Sarafidis P, Fernandez-Alfonso MS, *et al.* Global cardiovascular protection in chronic kidney disease. *Nat Rev Cardiol* 2016; 13: 603–608.
3. Townsend RR and Taler SJ. Management of hypertension in chronic kidney disease. *Nat Rev Nephrol* 2015; 11: 555–563.
4. Zhou L and Liu Y. Wnt/β-catenin signaling and renin–angiotensin system in chronic kidney disease. *Curr Opin Nephrol Hypertens* 2016; 25: 100–106.
5. Mann JF, Schmieder RE, McQueen M, *et al.* Renal outcomes with telmisartan, ramipril, or both, in people at high vascular risk (the ONTARGET study): a multicentre, randomised, double-blind, controlled trial. *Lancet* 2008; 372: 547–553.
6. Wolf G. Renal injury due to renin–angiotensin-aldosterone system activation of the transforming growth factor-β pathway. *Kidney Int* 2006; 70: 1914–1919.
7. Zhou L, Li Y, Hao S, *et al.* Multiple genes of the renin–angiotensin system are novel targets of Wnt/β-catenin signaling. *J Am Soc Nephrol* 2015; 26: 107–120.
8. Roager HM and Licht TR. Microbial tryptophan catabolites in health and disease. *Nat Commun* 2018; 9: 3294.
9. Sircana A, De Michieli F, Parente R, *et al.* Gut microbiota, hypertension and chronic kidney disease: recent advances. *Pharmacol Res* 2019; 144: 390–408.
10. Meijers B, Jouret F and Evenepoel P. Linking gut microbiota to cardiovascular disease and hypertension: lessons from chronic kidney disease. *Pharmacol Res* 2018; 133: 101–107.
11. Chen YY, Chen DQ, Chen L, *et al.* Microbiome-metabolome reveals the contribution of gut–kidney axis on kidney disease. *J Transl Med* 2019; 17: 5.
12. Cosola C, Rocchetti MT, Cupisti A, *et al.* Microbiota metabolites: pivotal players of cardiovascular damage in chronic kidney disease. *Pharmacol Res* 2018; 130: 132–142.

13. Cavalcanti Neto MP, Aquino JS, Romao da Silva LF, *et al*. Gut microbiota and probiotics intervention: A potential therapeutic target for management of cardiometabolic disorders and chronic kidney disease? *Pharmacol Res* 2018; 130: 152–163.
14. Hutkins RW, Krumbeck JA, Bindels LB, *et al*. Prebiotics: why definitions matter. *Curr Opin Biotechnol* 2016; 37: 1–7.
15. Chen DQ, Feng YL, Cao G, *et al*. Natural products as a source for antifibrosis therapy. *Trends Pharmacol Sci* 2018; 39: 937–952.
16. Chen DQ, Hu HH, Wang YN, *et al*. Natural products for the prevention and treatment of kidney disease. *Phytomedicine* 2018; 50: 50–60.
17. Chen YY, Yu XY, Chen L, *et al*. Redox signaling in aging kidney and opportunity for therapeutic intervention through natural products. *Free Radic Biol Med* 2019; 141: 141–149.
18. Chen L, Cao G, Wang M, *et al*. The matrix metalloproteinase-13 inhibitor poricoic acid ZI ameliorates renal fibrosis by mitigating epithelial-mesenchymal transition. *Mol Nutr Food Res* 2019; 63: e1900132.
19. Tian T, Chen H and Zhao YY. Traditional uses, phytochemistry, pharmacology, toxicology and quality control of Alisma orientale (Sam.) Juzep: a review. *J Ethnopharmacol* 2014; 158: 373–387.
20. Feng YL, Chen H, Tian T, *et al*. Diuretic and anti-diuretic activities of the ethanol and aqueous extracts of Alismatis rhizoma. *J Ethnopharmacol* 2014; 154: 386–390.
21. Chen DQ, Feng YL, Tian T, *et al*. Diuretic and anti-diuretic activities of fractions of Alismatis rhizoma. *J Ethnopharmacol* 2014; 157: 114–118.
22. Dou F, Miao H, Wang JW, *et al*. An integrated lipidomics and phenotype study reveals protective effect and biochemical mechanism of traditionally used Alisma orientale Juzepzuk in chronic renal disease. *Front Pharmacol* 2018; 9: 53.
23. Chen H, Yang T, Wang MC, *et al*. Novel RAS inhibitor 25-O-methylalisol F attenuates epithelial-to-mesenchymal transition and tubulo-interstitial fibrosis by selectively inhibiting TGF-β-mediated Smad3 phosphorylation. *Phytomedicine* 2018; 42: 207–218.
24. Chen L, Chen DQ, Liu JR, *et al*. Unilateral ureteral obstruction causes gut microbial dysbiosis and metabolome disorders contributing to tubulointerstitial fibrosis. *Exp Mol Med* 2019; 51: 38.
25. Tamaki H, Wright CL, Li X, *et al*. Analysis of 16S rRNA amplicon sequencing options on the Roche/454 next-generation titanium sequencing platform. *PLoS One* 2011; 6: e25263.
26. Bruce-Keller AJ, Salbaum JM, Luo M, *et al*. Obese-type gut microbiota induce neurobehavioral changes in the absence of obesity. *Biol Psychiatry* 2015; 77: 607–615.
27. Yang S, Liebner S, Alawi M, *et al*. Taxonomic database and cut-off value for processing mcrA gene 454 pyrosequencing data by MOTHUR. *J Microbiol Methods* 2014; 103: 3–5.
28. Cole JR, Wang Q, Fish JA, *et al*. Ribosomal Database Project: data and tools for high throughput rRNA analysis. *Nucleic Acids Res* 2014; 42: D633–D642.
29. Chen DQ, Feng YL, Chen L, *et al*. Poricoic acid A enhances melatonin inhibition of AKI-to-CKD transition by regulating Gas6/Axl-NF-κB/Nrf2 axis. *Free Radic Biol Med* 2019; 134: 484–497.
30. Chen DQ, Cao G, Chen H, *et al*. Identification of serum metabolites associating with chronic kidney disease progression and anti-fibrotic effect of 5-methoxytryptophan. *Nat Commun* 2019; 10: 1476.
31. Zhao YY, Wang HL, Cheng XL, *et al*. Metabolomics analysis reveals the association between lipid abnormalities and oxidative stress, inflammation, fibrosis, and Nrf2 dysfunction in aristolochic acid-induced nephropathy. *Sci Rep* 2015; 5: 12936.
32. Santisteban MM, Qi Y, Zubcevic J, *et al*. Hypertension-linked pathophysiological alterations in the gut. *Circ Res* 2017; 120: 312–323.
33. Jiang S, Xie S, Lv D, *et al*. Alteration of the gut microbiota in Chinese population with chronic kidney disease. *Sci Rep* 2017; 7: 2870.
34. Tain YL, Lee WC, Wu KLH, *et al*. Resveratrol prevents the development of hypertension programmed by maternal plus post-weaning high-fructose consumption through modulation of oxidative stress, nutrient-sensing signals, and gut microbiota. *Mol Nutr Food Res* 2018; 62: e1800066.
35. Chen L, Yang T, Lu DW, *et al*. Central role of dysregulation of TGF-β/Smad in CKD progression and potential targets of its treatment. *Biomed Pharmacother* 2018; 101: 670–681.
36. Nusse R and Clevers H. Wnt/β-catenin signaling, disease, and emerging therapeutic modalities. *Cell* 2017; 169: 985–999.

37. Yang T, Richards EM, Pepine CJ, *et al*. The gut microbiota and the brain-gut–kidney axis in hypertension and chronic kidney disease. *Nat Rev Nephrol* 2018; 14: 442–456.

38. Antza C, Stabouli S and Kotsis V. Gut microbiota in kidney disease and hypertension. *Pharmacol Res* 2018; 130: 198–203.

39. Felizardo RJF, Watanabe IKM, Dardi P, *et al*. The interplay among gut microbiota, hypertension and kidney diseases: the role of short-chain fatty acids. *Pharmacol Res* 2019; 141: 366–377.

40. Kanbay M, Onal EM, Afsar B, *et al*. The crosstalk of gut microbiota and chronic kidney disease: role of inflammation, proteinuria, hypertension, and diabetes mellitus. *Int Urol Nephrol* 2018; 50: 1453–1466.

41. Yang T, Santisteban MM, Rodriguez V, *et al*. Gut dysbiosis is linked to hypertension. *Hypertension* 2015; 65: 1331–1340.

42. Li J, Zhao F, Wang Y, *et al*. Gut microbiota dysbiosis contributes to the development of hypertension. *Microbiome* 2017; 5: 14.

43. Marques FZ, Mackay CR and Kaye DM. Beyond gut feelings: how the gut microbiota regulates blood pressure. *Nat Rev Cardiol* 2018; 15: 20–32.

44. Yan Q, Gu Y, Li X, *et al*. Alterations of the gut microbiome in hypertension. *Front Cell Infect Microbiol* 2017; 7: 381.

45. Ferguson JF, Aden LA, Barbaro NR, *et al*. High dietary salt-induced dendritic cell activation underlies microbial dysbiosis-associated hypertension. *JCI Insight* 2019; 5: e126241.

46. Durgan DJ, Ganesh BP, Cope JL, *et al*. Role of the gut microbiome in obstructive sleep apnea-induced hypertension. *Hypertension* 2016; 67: 469–474.

47. Marques FZ, Nelson E, Chu PY, *et al*. High-fiber diet and acetate supplementation change the gut microbiota and prevent the development of hypertension and heart failure in hypertensive mice. *Circulation* 2017; 135: 964–977.

48. Sharma RK, Yang T, Oliveira AC, *et al*. Microglial cells impact gut microbiota and gut pathology in angiotensin II-induced hypertension. *Circ Res* 2019; 124: 727–736.

49. Nogueira A, Pires MJ and Oliveira PA. Pathophysiological mechanisms of renal fibrosis: a review of animal models and therapeutic strategies. *In Vivo* 2017; 31: 1–22.

50. Nishiyama K, Aono K, Fujimoto Y, *et al*. Chronic kidney disease after 5/6 nephrectomy disturbs the intestinal microbiota and alters intestinal motility. *J Cell Physiol* 2019; 234: 6667–6678.

51. Yang J, Lim SY, Ko YS, *et al*. Intestinal barrier disruption and dysregulated mucosal immunity contribute to kidney fibrosis in chronic kidney disease. *Nephrol Dial Transplant* 2019; 34: 419–428.

52. Lau WL, Vaziri ND, Nunes ACF, *et al*. The phosphate binder ferric citrate alters the gut microbiome in rats with chronic kidney disease. *J Pharmacol Exp Ther* 2018; 367: 452–460.

53. Zhang ZH, Wei F, Vaziri ND, *et al*. Metabolomics insights into chronic kidney disease and modulatory effect of rhubarb against tubulointerstitial fibrosis. *Sci Rep* 2015; 5: 14472.

54. Zhang ZH, Vaziri ND, Wei F, *et al*. An integrated lipidomics and metabolomics reveal nephroprotective effect and biochemical mechanism of Rheum officinale in chronic renal failure. *Sci Rep* 2016; 6: 22151.

55. Zhang ZH, Li MH, Liu D, *et al*. Rhubarb protect against tubulointerstitial fibrosis by inhibiting TGF-β/Smad pathway and improving abnormal metabolome in chronic kidney disease. *Front Pharmacol* 2018; 9: 1029.

56. Chen H, Yuan B, Miao H, *et al*. Urine metabolomics reveals new insights into hyperlipidemia and the therapeutic effect of rhubarb. *Anal Method* 2015; 7: 3113–3123.

57. Zeng YQ, Dai Z, Lu F, *et al*. Emodin via colonic irrigation modulates gut microbiota and reduces uremic toxins in rats with chronic kidney disease. *Oncotarget* 2016; 7: 17468–17478.

58. Yang F, Huang XR, Chung AC, *et al*. Essential role for Smad3 in angiotensin II-induced tubular epithelial-mesenchymal transition. *J Pathol* 2010; 221: 390–401.

59. Feng YL, Chen DQ, Vaziri ND, *et al*. Small molecule inhibitors of epithelial-mesenchymal transition for the treatment of cancer and fibrosis. *Med Res Rev* 2019; 40: 54–78.

60. Hu HH, Chen DQ, Wang YN, *et al*. New insights into TGF-β/Smad signaling in tissue fibrosis. *Chem Biol Interact* 2018; 292: 76–83.

61. Wang M, Chen DQ, Chen L, *et al*. Novel inhibitors of the cellular renin–angiotensin system components, poricoic acids, target Smad3 phosphorylation and Wnt/β-catenin pathway

against renal fibrosis. *Br J Pharmacol* 2018; 175: 2689–2708.

62. Wang M, Chen DQ, Wang MC, *et al*. Poricoic acid ZA, a novel RAS inhibitor, attenuates tubulo-interstitial fibrosis and podocyte injury by inhibiting TGF-β/Smad signaling pathway. *Phytomedicine* 2017; 36: 243–253.
63. Wang M, Chen DQ, Chen L, *et al*. Novel RAS inhibitors poricoic acid ZG and poricoic acid ZH attenuate renal fibrosis via Wnt/β-catenin pathway and targeted phosphorylation of smad3 signaling. *J Agric Food Chem* 2018; 66: 1828–1842.
64. Chen DQ, Cao G, Zhao H, *et al*. Combined melatonin and poricoic acid A inhibits renal fibrosis through modulating the interaction of Smad3 and β-catenin pathway in AKI-to-CKD continuum. *Ther Adv Chronic Dis* 2019; 10: 2040622319869116.
65. Xu P, Liu J and Derynck R. Post-translational regulation of TGF-β receptor and Smad signaling. *FEBS Lett* 2012; 586: 1871–1884.
66. Yang T, Chen YY, Liu JR, *et al*. Natural products against renin–angiotensin system for antifibrosis therapy. *Eur J Med Chem* 2019; 179: 623–633.
67. Liu D, Chen L, Zhao H, *et al*. Small molecules from natural products targeting the Wnt/β-catenin pathway as a therapeutic strategy. *Biomed Pharmacother* 2019; 117: 108990.
68. Chen L, Chen DQ, Wang M, *et al*. Role of RAS/Wnt/β-catenin axis activation in the pathogenesis of podocyte injury and tubulo-interstitial nephropathy. *Chem Biol Interact* 2017; 273: 56–72.